

**ANALYSIS OF SOIL PILE INTERACTION**

(also lateral load analysis)

**A REPORT  
IN PARTIAL COMPLETION OF REQUIREMENT SUBMITTED FOR THE AWARD  
OF THE DEGREE  
OF  
MASTER OF TECHNOLOGY  
(GEOTECHNICAL ENGINEERING)**

by:

**POONAM KUMARI**

(2K19/GTE/20)

Supervised by:

**Prof. NARESH KUMAR**



**DEPARTMENT OF CIVIL ENGINEERING  
DELHI TECHNOLOGICAL UNIVERSITY  
(Formerly Delhi College of Engineering  
Bawana Road, Delhi-110042**

**JULY, 2021**

**DELHI TECHNOLOGICAL UNIVERSITY  
(Formerly Delhi College of Engineering)  
Bawana Road, Delhi-110042**

**CANDIDATE'S DECLARATION**

I, Poonam Kumari, a 2K19/GTE/20 Master of Technology (Geotechnical Engineering) student, hereby confirm that the project Thesis labelled "Soil Pile Interaction (also analysis of lateral load)" that I filed to the Department of Civil Engineering, Delhi Technological University, Delhi in achievement of the requirements for the degree of Master of Technology, is original and complete and this work has not be used to grant a degree, diploma associateship, fellowship, or other comparable honour.

**Place: Arunachal Pradesh**

**Poonam Kumari**

**Date: 3 AUGUST**

**DEPARTMENT OF CIVIL ENGINEERING**  
**DELHI TECHNOLOGICAL UNIVERSITY**  
(Formerly Delhi College of Engineering)  
Bawana Road, Delhi-110042

**CERTIFICATE**

I, the undersigned, hereby attest to the fact that the Project Research paper titled "soil pile interaction(lateral load analysis)" submitted by Poonam Kumari, Roll No 2K19/GTE/20 [Department of Civil Engineering], Delhi Technological University, Delhi in fulfilment of the requirements for the requirement for the award of Master of Technology, is a document of the major project carried out by student under my guidance.

PLACE: Arunachal Pradesh

DATE: 3 AUGUST

Prof. Naresh Kumar

Supervisor

## ACKNOWLEDGEMENT

It is indeed a great pleasure and privilege to present this report of Major Project -1 titled “Soil pile interaction (analysis of lateral load)” under the guidance and supervision of **Prof. Naresh Kumar** .

I, Poonam Kumari (2K19/GTE/20) want to convey my sincere gratitude to **Prof. Naresh Kumar** for supporting me throughout the project. His patience, helpful information, insightful comments, practical advice and motivation have tremendously helped me in the research work. Without his guidance and support, this project would have not been completed.

In the times like this where whole world is fighting with the pandemic of COVID-19, I feel really blessed and thankful to my supervisor for his kind and helpful nature that helped and eased out the working of this project.

**Poonam Kumari**

## CONTENT

Candidate's Declaration  
Certificate  
Acknowledgement  
List of figure  
Abstract  
Introduction  
Proposed BEM Based method  
Validation of proposed method  
Conclusion  
Rerences

## List of Figure

- Figure 1: discretization of a pile
- Figure 2: shows a solution plan for the mindlin problem.
- Figure 3: pile group interaction system with mobilised soil passive wedges
- Figure 4: lateral interaction for one of the group's piles
- Figure 5: soil pressure profile
- Figure 6: Shadow modelling for the pile group effect
- Figure 7: Soil pressure profile as a result
- Figure 8 : A suggested nonlinear adaptive step size method
- Figure 9 : adaptive step size control
- Figure 10: horizontal load measured vs. calculated
- Figure 11 : bending moment curvature relationship in a pile section
- Figure 12: calculated vs. measured result
- Figure 13: Load deflection curve calculated vs. measured
- Figure 14: Group efficiency calculated vs. measured
- Figure 15: Deflection profile calculated vs. measured

## **ABSTRACT**

Boundary Element Method progress into research for study pile groups. This method including the non-linear conduct of the soil by a hyperbolic modulus reduction curve; the non-linear response of rc pile section. The non-linear behaviour of soil is modelled using a hyperbolic modulus reduction curve; the non-linear response of rcc pile sections is modelled using a hyperbolic modulus reduction curve, also considering tension stiffening's impact; and the effect of suction is modelled using rising the stiffness of shallow portions of soil. The pile group shadowing effect was analysed by a method comparable to that suggested in the Strain Wedge Model for pile group studies. In comparison to more complicated codes like VERSAT-P3D, PLAXIS 3D, and FLAC-3D, the suggested BEM approach requires less computing effort and produces accurate results utilising data from a normal site inquiry. A study of measured and calculated result for a horizontal loaded fixed-head pile group made up of rcc bored piles is provided. The findings of the recommended approach are found to be quite similar to those obtained in the field. To determine the ultimate lateral capacity and deflection under working loads, all tests were carried out to failure. When compared to straight shaft piles, test findings show a non linear response, a significant increase in lateral capacity, and a reduction in deflections at working loads.

## INTRODUCTION

Many study has focused on the response of stack bases to horizontal stress, from a single stack to advance through stack groups to combined stacked surfaces at last. But more experior research is required to understand the relationships between soil, piles and superstructures such as Mokwa & Duncan, Katzenbach and Turek, as many authors have pointed out. The constraint conditions of the stackhead and the relative rigidity of the stack soil are very significant factors that influence the response in any stack scenario [3] and [4] have done extensive experiments with laterally charged pile groups, but the reality is that the pile-to-surface interactions, and the stiffness of the connection structure compared with the single pile case, are further considerations.

The pile-heads are constantly deflected under lateral pressure across all piles.

On the other hand, BEM techniques treat soil as homogenous elastic half-space with a  $E$  and  $\mu$ , enabling direct assessment of the Interactions between soil and piles, as well as group impacts, allowing for pile groups and the piles-rafts analysis. Their results may also be considered.



## 1. Submitted method 'BEM-Based'

### 1.1. Key characteristics of the proposed method

For pile-group analysis, non-linear methods must reconstruct the important linkages between foundational components and the soil. The ability of this proposed method to provide a complete soil continuum BEM analysis with all interactions is the unique factor. In terms of limit values, BEM addresses the issue completely.

This resulted in a considerable reduction in the number of unknowns for which considerable time savings and data preparation effort had to be resolved. For issues with three dimensions, stack groups. The nonlinear soil response is modelled in custom category of an almost hyperbolic elastic drop curve formulation by Fahey and Carter . Following are presumption which underlie the technique:

a) The solution of Mindlin is used to consider interactions of pile-surface and pile-pile; b) the elastic horizontal layer; c) the nonlinear compliance of the reinforced concrete pile section; d) the comportement of the unlinear terrain (incremental analysing) .

In accordance with the connection provided the final soil pressure profile is assessed.

## 1.2. Modeling of piles

The stack is shown as a vertical line with a length and depth of 60 blocks, and the geometrically specified external diameter  $D$  and length  $L$  of the real stack.

This discretization may decrease the calculation time. This discretization may decrease the calculation time.

Figure 1 depicts the discretization :

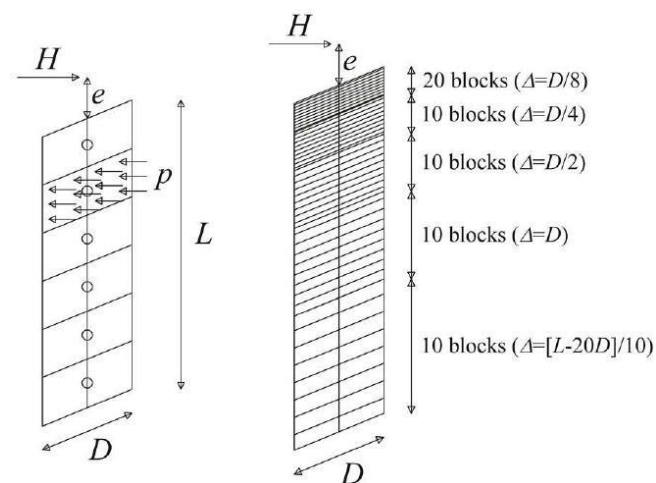


Figure 1 pile discretization

- 20  $D/8$  thick blocks starting from ground level and working at  $2.5D$  depths,
- 10  $D/4$  thick blocks working at depth of  $5D$ ,
- 10  $D/2$ , working up to  $10D$  depths,
- 20  $D/8$  thick blocks starting from ground level and working up to  $2.5d$  depth;
- 10  $D/4$  thick blocks working to  $D/4$  thicknesses;
- 20 blocks working up to a  $D/5$  thickness of depth, pile foundation depth.

In response to numerous parametric investigations, Landi[21] suggested that the criteria of discretization be defined. The authors used the same stack modelling provided here to investigate the side effect of a single stack[22]. In this article, the authors mentioned some particular characteristics of pile modelling that may also be found to help the reader comprehend the text[22] in general.

For pile-group analysis, non-linear methods must reconstruct the important linkages between foundational components and the soil. The ability of this proposed method to provide a complete soil continuum BEM analysis with all interactions is the unique factor. In terms of limit values, BEM addresses the issue completely, especially at the pile-soil interface

$i$

The lateral movement of each pile

$$y_i = \sum_{j=1}^n a_{ij} P_j + y_0 + \theta_0 z_i$$

$y_0$  and  $\theta_0$  are the unknown pile-head displacement and rotation,  $P_j$  indicates for pile-block  $j$  load in particular (placed at depth  $z_j$ ). The  $n + 2$  unknown function (or  $1 n +$  for circumstances), and the  $n + 1$  pile interface pressures, is a function of each pile point displacement.

The steel pipe and concrete reinforced piles are analysed utilising the suggested technique. In the study of steel plates, bending rigidity  $E_p I_p$  is constant. Even at low bending moment values, fracture formation in reinforced concrete sections requires a distinct pile reaction model. The relationship between "curvature-stroke-axial load," which also accounts for tension intensification, is computed using this model [23].

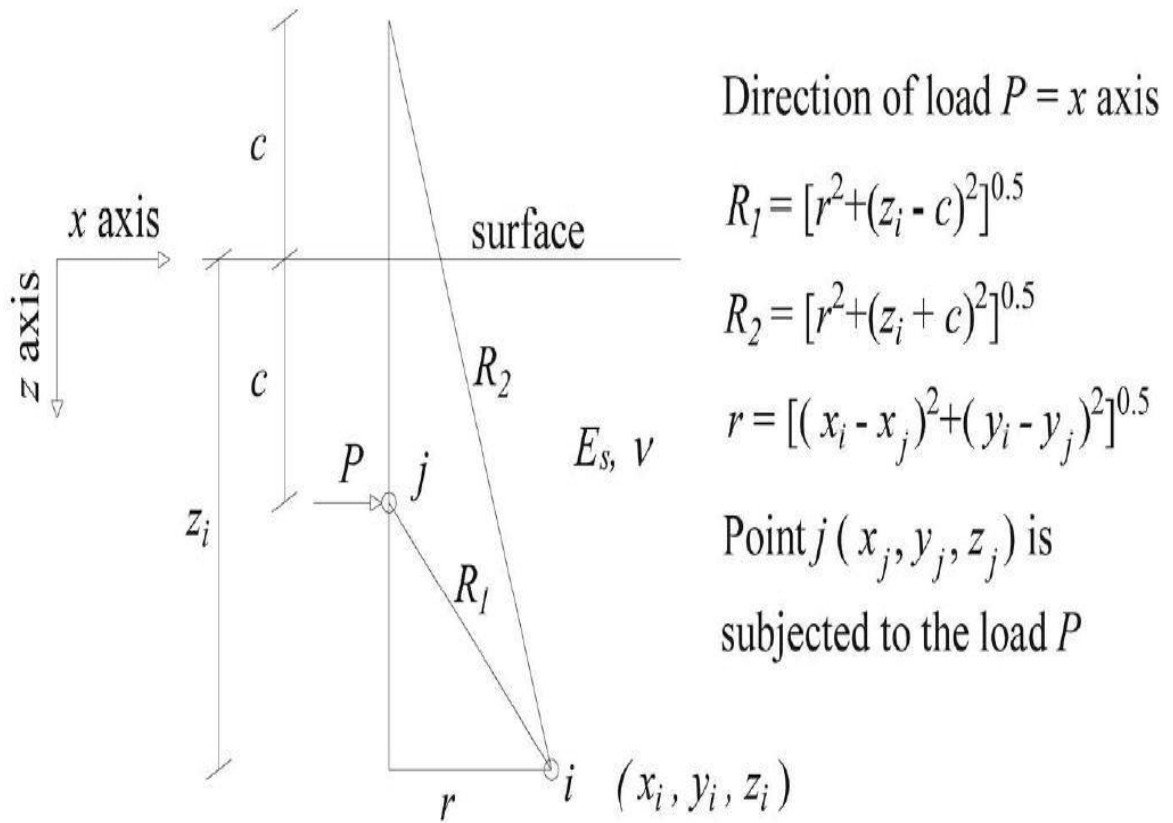
This model is presented in full in [23], but it is an extension of another model which analyses the stiffening tension effect in the circular section for rectangular armoured concrete.

Once a time-curvature A connection has been created,  $E_p I_p$ , the coefficients of the flexibility matrix for rc pile modelled a step-taped beam with a changeable flexural stiffness, along the pile shaft, must be specified.

The difference between  $E_p$  and  $I_p$  on the shaft is considered completely replacing the  $I_p$  of segment although maintaining  $E_p$  steady. Incremental analysis must modify the pile flexibility matrix at each load increment.

### ***1.3. Modeling of soil***

The ground is designed as an elastic half-space with many layers. BEM analysis involves the integration on the surface of the issue domain of a suitable elementary singular solution. The solution evaluating interactions between piles and soil is only valid and strict in cases of homogeneous elastic half space, but in event of multi-faceted elastic half-space still be regarded as valid by Poulos and Davis is utilised in the present research, such that a soil elastic module inserted in Mindlin equation is the average value between the elastic module in evaluating position and flexible module in the application of force.



The horizontal displacement  $s_{ij}$  at the point  $i$  due to the load  $P$  applied at point  $j$  is obtained with Equation (4)

**Figure 2.** Mindlin solution scheme.

#### 1.4 Soil non linear behaviour

In [22-25], curves for shear stress-stretching have been resemble by hyperbolae with a  $G_{max}$ -equivalent tangent at zero strain.

The hyperbola equation may be rewritten standardised secant shear modulus ( $G$ ), which decreased with a normalised shear strain by specifying the reference strain ( $\mu_g = \epsilon_{max} = G_{max}$ ).

The non-linear conduct of soil was represented using a modified Fahey and Carter's wording [17].

" Only the horizontal stresses are expected to change during the vertical stress analysis during the lateral load analysis . The "shear stress-to-most-shear stress" ratio is thus analogous to the "p/pult/to-shear stress" ratio (p/pult/to-shear stress/shear strength ratio [17])

A Equations of soil- and pile displacement compatibility as well as translation equations and rotations balance, are required in the resolution scheme and are distinctive in BEM methods (at the pile-heads, employing suitable boundary conditions). For the instances of head stack . The analysis is gradually performed, with a step-by-step adaptive control.

### 1.5. Suction impact on the Pile Group in reaction to side loading

Suction is essential element of the lateral stresses of the pile foundation since its reactions are mostly influenced by the less shallow soil layers.

The method presented is founded on "MK-Model" conceived by Aubertin et al. [28] (modified-kovacs model). This model uses component. Suction is essential element in a pile foundation that is subjected to horizontal loads since response of foundation system is largely impacted by shallower soil layers. The suggested technique employs the "MK-Model" proposed the (Modified-Kovacs Model). [28] In this model, the corresponding capillary rise  $h_{c0}$  is used as a parameter. This parameter serves same purpose as average capillary rise in Kovacs' model, computed through equation.

$$h_{c0}(cm) = \frac{0.75}{e \cdot D_{10}[1 + 1.17 \cdot \log C_u]}$$

The model assumes, water kept in place by capillary forces, for the degree of saturation, the MK-Model proposes the following relationship

$$S_r = \frac{\theta}{\theta_s} = S_c + S_a^* \cdot (1 - S_c).$$

### 1.6. Group Effects Assessment

Results indicate that the interaction between stacks in many rows cannot be assessed for short distance values simply by taking into consideration .

The motion of the front piles generates an active condition almost instantly.

This reduces both the rigidity and resistance of the soil causing the back heaps to react. This required a means of better capturing the behaviour seen in the experimental information using the suggested BEM approach. A similar approach we employed was described in [16].

According to th latterresearch, interaction between heaps is determined by assumed shape of passive wedge in front of pile and pile spacing.

Fig. 4 shows overlap of wedges at general depth z of neighbouring piles.

The load of the inner piles in each line is smaller than the weight of the outer piles. This was discovered in a series of tests published in[16].

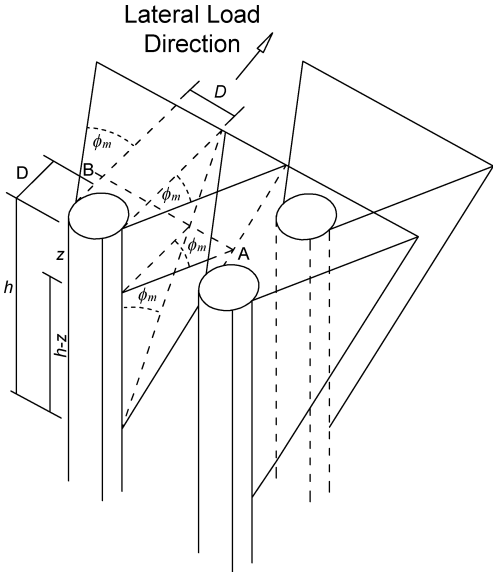


**Figure 3.** Pile-group interaction system with mobilised soil passive wedges (in the same way the so Strain Wedge Model is described [16]).

There are therefore greater levels of soil strains and stresses at a certain depth



(Figure3) than isolated piles in overlapping areas[16]. The increase in average soil reaction of a pile's passive coil is calculated by the unit and extent of interfering coils the pile's edges are overlapping coil (Figure4)

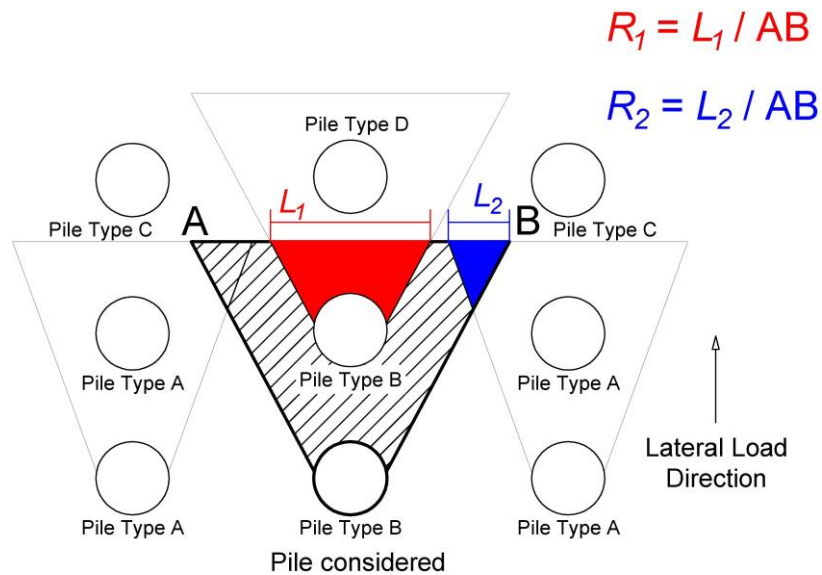


**Figure 4.** For a specific pile in the group, there is lateral interaction [16]

This overlap is based on the grouping location of the stack.

The mean stress level in the earth's layer is derived using an analytical relation, which provides excellent agreements with field test data[16]. The result of passive wedge interference.

$$SL_g = SL_i \cdot 1 + \sum R_j \leq 1$$

$j$  = number of neighbouring passive wedges overlapping the pile wedge;

$R$  = ratio of length of overlapping part of passive wedge face ( $L$ ) to the overall face length of passive wedge ( $AB$ );

$R_j$  computed from neighbouring pile pile .

The  $SL_i$  value on right side of following equation represents the  $SL$  in Strain Wedge Model of an isolated stack for cohesive soils as set forth in Equation.

$$SL = \frac{\Delta\sigma_h}{\Delta\sigma_{hf}} = \tan^2 \left( 45^\circ + \frac{\phi}{2} \right) - 1$$

where  $\Delta\sigma_{hf}$  is the lateral stress variation at failing

$$\Delta\sigma_{hf} = \sigma_{v0} \tan^2 \left( 45^\circ + \frac{\phi}{2} \right) - 1 .$$

However, it is stated in the proposed approach that  $SL_i \cong p/p_{ult}$ , thus

the mobile resistance angle,  $m$ , may easily be computed if  $SL_i$ , which is supposed to be equivalent to the  $p/p_{ult}$  ratio is known. The  $SL_g$  levels fluctuate according on loading depth and quantity. The pressure rise at each contact of the pile-soil may be determined using them ( $pg$ )

However, it is assumed that they will not be drained in case of cohesive soils. The value thus equal to 0 and  $m$  is always equal to 0. For cohesive soils the base angle will always be 45 degrees, and only the passive wedge's depth (and therefore

plain) dimension changes as the load increases. However, it is possible to look just at the interaction between the pile wedge in the front line and the pile wedge before it and thus to disregard the interact with the pile wedges in the same row (Figure6).

The extreme case of piles row with a relative distance  $s/D$  of 1 is investigated in order to overcome this restriction and the interactions between heap wedges positioned side by side are thus considered. The final profile of soil resistance should in theory be the same as for a retention wall, determined by the difference in undraining situation between passive and active earth pressure.

$$p_a(z) = [\sigma_{v0}(z) - 2c_u(z)] \cdot D = [\gamma \cdot z - 2c_u(z)] \cdot D$$

$$p_p(z) = [\sigma_{v0}(z) + 2c_u(z)] \cdot D = [\gamma \cdot z + 2c_u(z)] \cdot D$$

It's important to note that the  $p_a$  value may be negative at low depths, showing that the ground is intensive. The difference between passive pressure and active pressure indicate that final ground pressure profile,  $P_r$ , operating in a row of 1D piles (force units per unit length) down the pile shaft (or on retention walls) In the calculation of the transverse pressure , for cohesive terrestrial fixed  $c_u$  of 50 kPa Figure7 illustrates all these stages.

20 kN/m<sup>3</sup> unit weight and 1 m battery width.

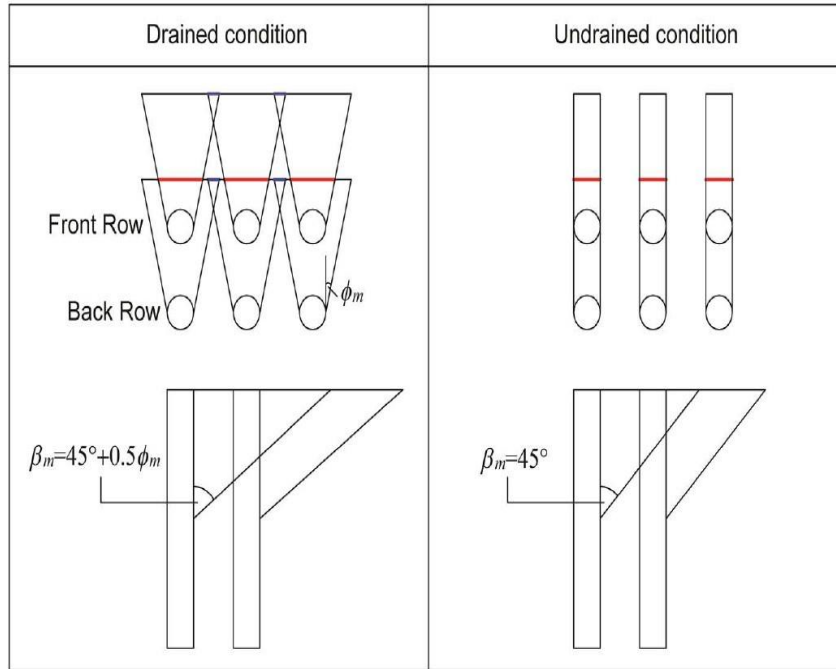


**Fig 6.** Pile group effect: shadowing modeling.

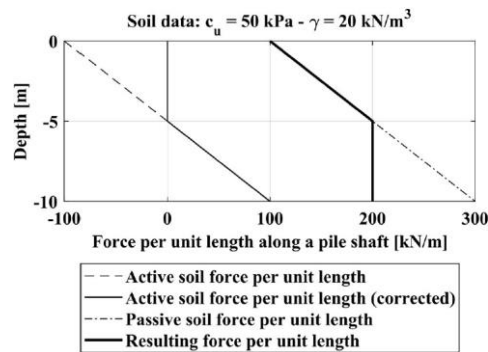


**Fig 5.** Soil pressure profile.

Soil resistance profile, according to the Matlock[18], is now taken into account pile terrain and represents lowest value for the same soil condition as before.

$$\text{Min} \left( 3 + \frac{\gamma J}{c_u} z + \frac{J}{c_u} z^2 \quad c_u; 9c_u D \right)$$

Compare pr (for 1D distances) and pult findings in Figure 7. (for an isolated solitary pile). According to all the analysed experimental data, the final soil resistance profile for the individual separated only applies to pile separation  $s/D$

to section 6.

The ultimate soil resistance ratio is believed to be intermediate between the profile  $p_r$  (assumed to be the distance ratio  $D = 1$ ) and the profile  $p_{ult}$  (assumed to be the distance between  $s / D$  and  $T / 6$ ). for pile separation ratio of less than 6.

The definitive soil resistance pattern ( $p_{ult,def}$ ) for spacing ratios between 1 and 6 is assumed to be a mix of the real  $s/D$  and the depth of  $z$  by formulation.

$$p_{ult,def}(z) = p_r(z) + F(s/D) \cdot (p_{ult}(z) - p_r(z))$$

where  $F(s/D)$  is a factor by Equation,

$$F(s/D) = \frac{s/D - 1}{5}$$

It may be examined by using this method, even for cohesive soils under unwet circumstances, to interact with piles located on side , simply replacing the ultimate soil resistance calculated by formulae of Matlock[18]

The mobilised solar passive wedge starts to develop at a depth through the pile shaft, varying from pile to pile, when pressure at interface changes from positive value to negative one from active to passive state.

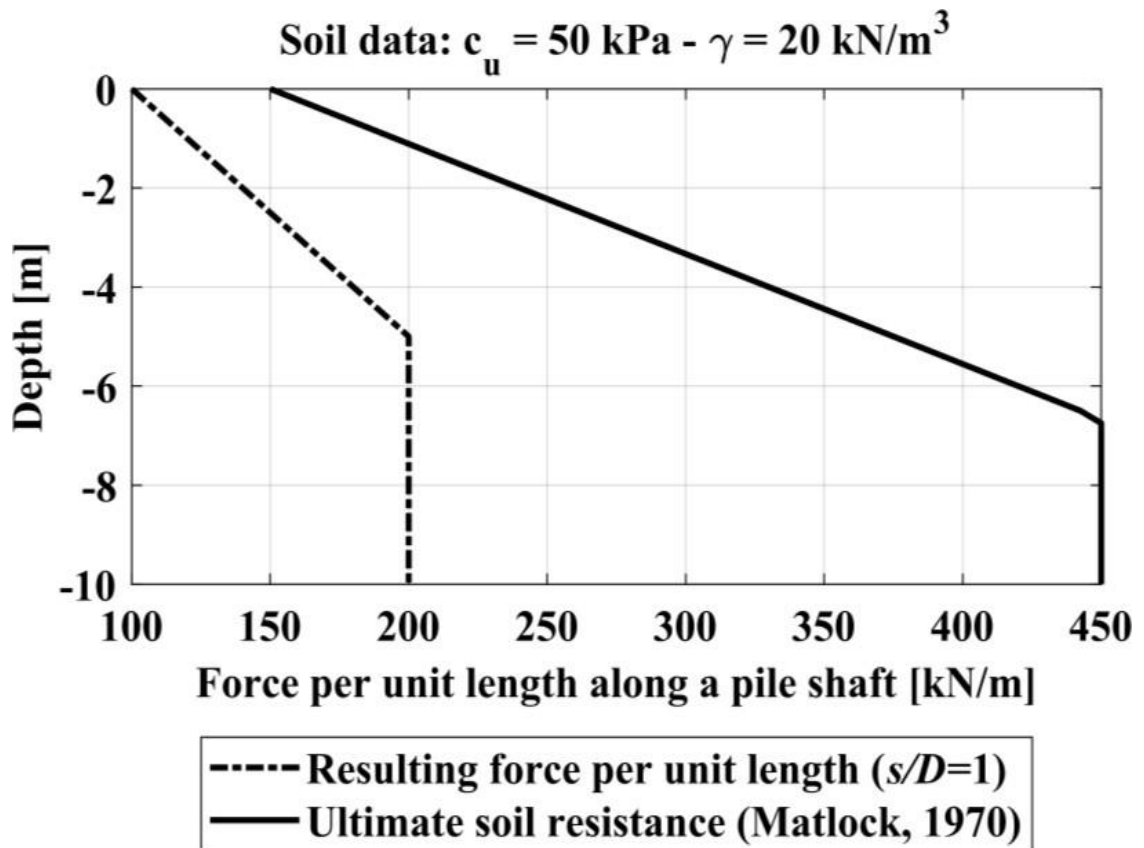


**Figure 7.** Resulting soil pressure profile

### 1.7 System Solution

Solution system:  $[F][X] = [P]$ .

Solution system (X) is an unknown vector of  $2m + 1$  or  $1 \text{ km} + 1$  terms for either pile or head conditions; where  $m$  is the number of piles,  $k$  are the number for each stack of pile,  $p$  is the kilometre of unknown pile pressures at a pile-soil interfaces,  $y_0$  is the pile-group displacement,  $m$  pile-head rotations,  $H_m$  are the  $m$  horizontal load of the pile-heads and  $[P]$  is the unknown pile-heads vector of  $\text{km} + 2m + 1$  terms or kilometre + 1 terms for free or fixed head circumstances, as the case may be; (with the same dimension as for the vector  $[X]$ ).  $[f]$  is (km

+  $2m + 1$ ) a string of kilometres +  $2m + 1$ ) or  $(km + m + 1)$  a string of a string of kilometres +  $m + 1$ ).

- kilometres/kilometers of flexibility matrix [FP], consisting of the pile-soil interface  $j$  to the pile-soil interface  $I$  which consists of the kilometres of the pile-soil Flexibility matrix [FS], comprised of kilometres of flexibility matrix [KM]

For the equilibrium imposition and completion of the compatibility equations at every node,  $H$  is horizontal load applied and  $f$  is excentricities of charge.

The flexibility matrix [F] is updated at each stage of the procedure. The pile flexibility sub-matrix [FP] is easily adjusted in event of a non-linear "moment-curvature" relation for pile section. The [FP] is updated using tangent flexural rigidities in line with bending moments achieved at each pile node during the preceding load increase. The flexibility matrix [F] is updated at each stage of the procedure. The pile flexibility sub-matrix [FP] is easily adjusted in the event of a non-linear "moment-curvature" relation for the pile section. The [FP] is updated using tangent flexural rigidities in line with bending moments achieved at each pile node during the preceding load increase.

The entire lateral load is applied in first stage process after original flexibility matrix [F] is calculated. Each generic charge increase takes place with two

solution. The first one uses  $h_k$  as load growth, the second one uses two loading stages is  $h_k/2$ . Figure 9 outlines repetitive arrangement. This corresponds to explicit Euler method for simplicity, with step-doubling control and adaptive step-size control. It may also be utilised to enhance the solution accuracy by using a fourth order Runge-Kutta technique. Press et al. [24] describes completely the adaptive step-size numerical control technique.



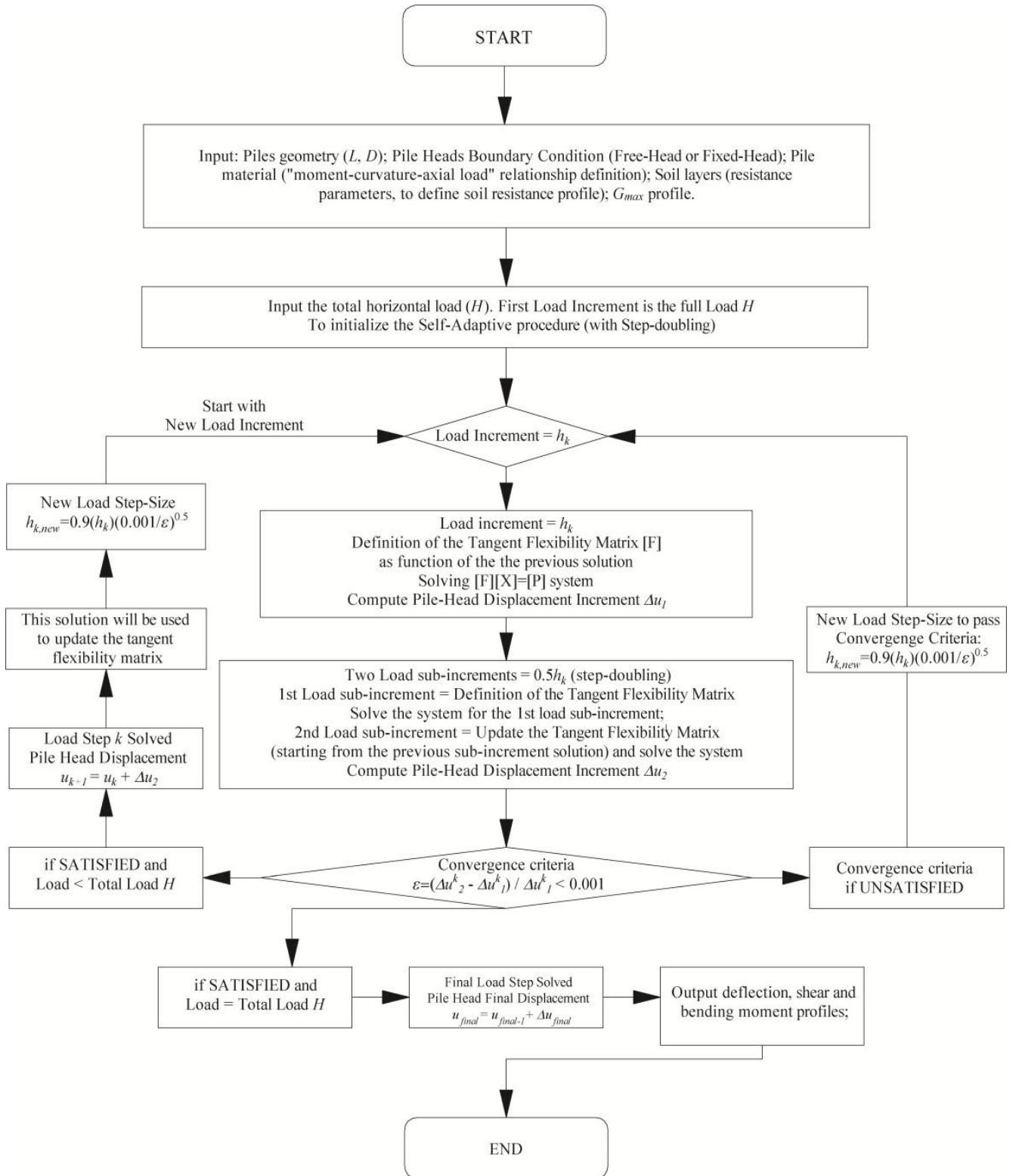


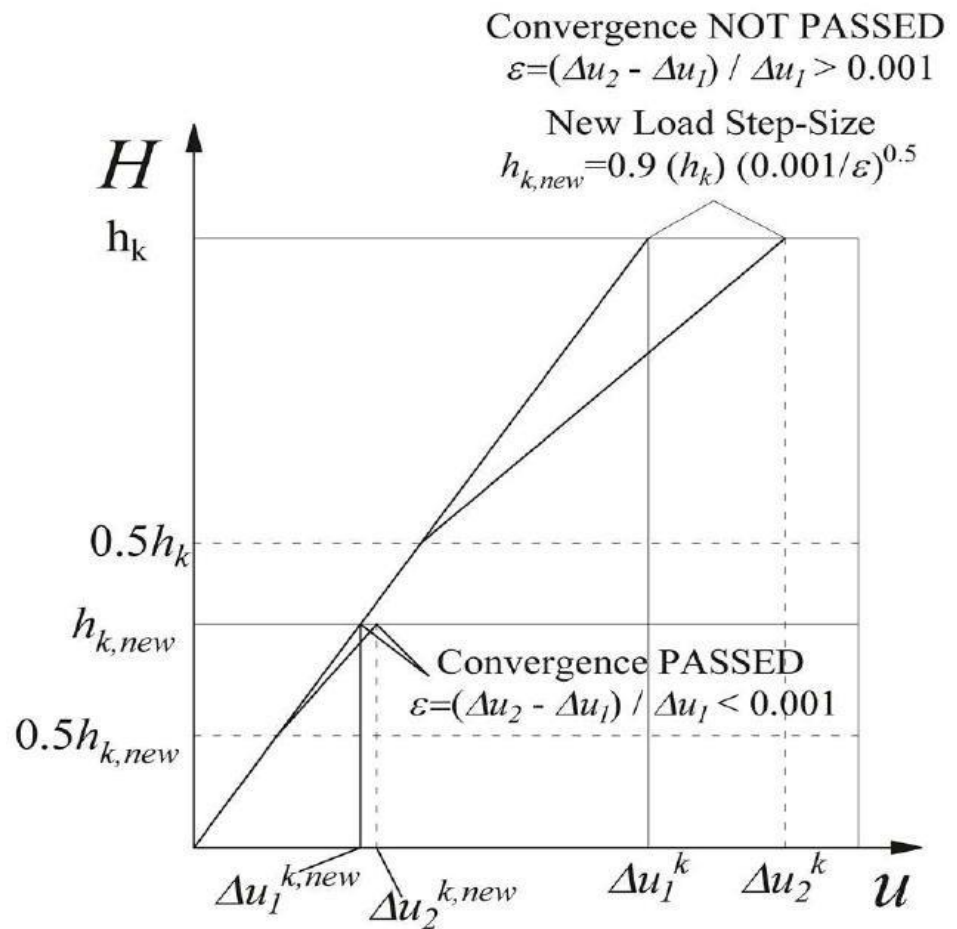
**Figure 8.** Flow chart of the proposed non-linear adaptive step-size method.

Following the computation of these two solutions, the incremental ratio is

calculated according to

$$\varepsilon = \frac{\Delta u_2 - \Delta u_1}{\Delta u_1}$$

where  $u_1$  and  $u_2$  are the one-step and two-step incremental displacements at the pile-head, respectively, figure compared to a predetermined tolerance of



0.001 percent. (Figure9)

**Figure 9.** Adaptive step-size control.

After threshold was surpass ( $\beta > \text{tol}$ ), an updated load increase  $h_{knew}$  will begin the iterative process again, enabling it to reach the required accuracy [24].

If this criteria is passed in the convergence process, Equation (24) will be used to evaluate the next step-size again. The next step is the convergence criterion. When the horizontal load  $H$  is achieved, process ends. Finally, the whole load-deflexion curve and the pile-soil interface pressure profile of the pile shaft may be assessed at each load stage.

Validation of the method proposed :

Result of stack group analysis utilising BEM method described in article are given in this section. These are compared to the findings obtained on sandy and cohesive plastic pile group pile load testing. Both on steel and r.c. piles lateral load test performed. The experimental results were obtained from well-recognized test on 15 stack groups, given in Table1.

**Table 1.** Case histories studied

Case Reference	Material	Diameter (m)	Length (m)	Soil	$H_{MAX}$ (kN)
[51] $3 \times 3; s = 3D$	Steel with	0.27	13.1	OC Clay	695
[4] $3 \times 2; s = 3D$	Grout-fill	3	1	Sand	808.
[8] $\phi' = 39^\circ; 3 \times 3;$ $s = 3D$	Bored RC	0.27	13.1	Silty	5
[8] $\phi' = 39^\circ; 3 \times 3;$ $s = 5D$	Aluminum	3	1	Sand	1104

The goal of analysis is to prove that BEM technique described in this work is correct. A young modulus determined from in situ testing at the low strain level is the soil elastic modulus to be considered.

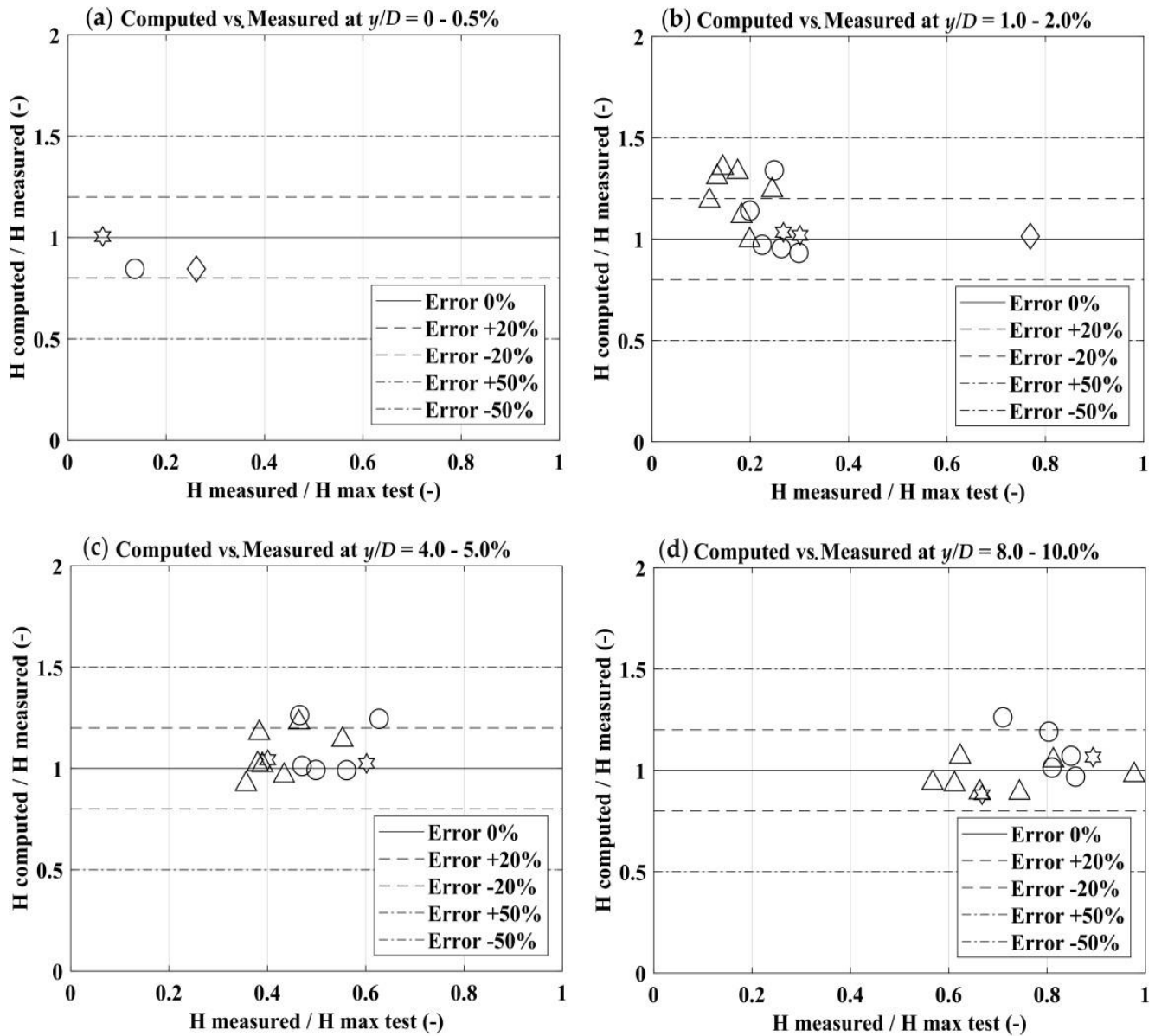
The proper  $g$  value to be entered may simply be assessed to get best match with horizontal pile load deflection curve. The input data utilised for analysing using the suggested technique were given in Table2. These statistics relate to characteristics of soil at least between the soil surface and the depth of 10 diameters.

**Table 2.** The input data that utilised to run analysis using the proposed technique.

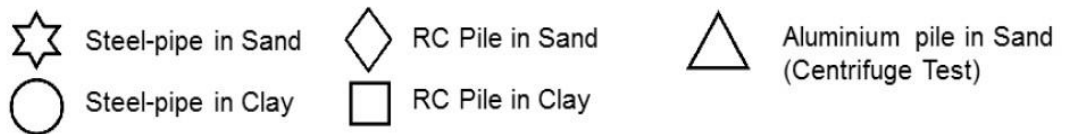
Case	EpIp	Y(KN/m <sup>3</sup> )	$\phi$	DR(%)	Cu(KPa)	$E_{max}$ (linearly increasing with Depth) (MPa)	G	F(m)	WT(m)	pile head B.C
[51]	16.0	19.0	-	-	58–145 (0–5.5 m)	70–200 (0–5.5 m)	0.25	0.305	0.0	Free
[5]	16.0	19.5	47	90	-	35–100 (0–2.0 m)	1.0	0.305	0.0	Free
[4]	variable	18.5	34	50	-	40–400 (0–34.9 m)	0.5	1.0	1.0	Fixed
[8]	72.1	14.51	34	33	-	60–300 (0–13.3 m)	0.25	1.68	-	Free
[8]	72.1	15.18	39	55	-	50–260 (0–13.3 m)	0.5	1.68	-	Free
[52]	514.0	16.3	40	89	-	40–200 (0–12.0 m)	1.0	1.6	-	Free
[53]	26.91	19.0	-	-	-	60–170 (0–8.7 m)	0.25	0.4	0.0	Free
[11]	30.03	19.5	40	44	-	20–150 (0–11.5 m)	0.25	0.86	0.0	Free
[54]	30.03	19.0	-	-	-	50–60 (0–4.0 m)	0.25	0.48	1.0	Free

Table Notes: EpIp = pile-strength,  $\beta$  = weight of a soil unit.  $\alpha$  = peak angle of friction. DR = density of shear; Emax = modulus elastic of a soil at a small strain level. f = eccentricity of load. Head B.C. = circumstances for pile-head border (free or fixed ).

When contrasting the calculated and measured results (Fig 10) shows that the suggested BEM approach is capable of providing the pile groups with excellent predictions of side responses.



**Legend:**



**Figure 10.** Measured vs. computed horizontal loads ( $H$ ) for a given normalized displacement ( $y/D$ ): (a)  $y/D = 0-0.5\%$ ; (b)  $y/D = 1.0-2.0\%$ ; (c)  $y/D = 4.0-5.0\%$ ; (d)  $y/D = 8.0-10.0\%$ .

### ***1.8 Analysis results of the proposed BEM Bored Pile Test method for a particular lateral load test***

In 2001, Taiwan implemented lateral charge test program[2]. Two sets of piles were subjected to horizontal load testing, one consisting of bored piles and other of driven piles. Tests performed using the same two methods on single piles placed. All the findings shown in this section relate to the single stack that is bored without the head and the group of bored stacks. The latter is a pile group of three to two (3 rows and two columns) at 3D distance.

### ***1.9 Properties of soil and pile Description***

The site categorised as silt or silty sand, with sometimes silty clay layers. The water table stood 1.0 m below the surface of the earth and throughout the whole testing period did not fluctuate significantly.

13 cast boring batteries and 13 precast driving batteries were installed on-site. The bentonite-slurry reversed circulation was used to make 11 of the 13 piles drilled ( $D = 1500\text{mm}$ ,  $L > 34.91\text{ m}$ ;  $EI > 6.862\text{ GNm}^2$ ). Two out of the 13 drilled piles were built using a full-length hydraulic oscillator drilling equipment. Measuring tools were connected to the longitudinal bars of reinforcement (strain gauges and slopes) placed in the hole before casting the concrete. Table 3 summarises the boring pile characteristics.

**Table 3.** Structural properties of bored pile.

<b>Pile Diameter</b> <i>D</i> (mm)	<b>Pile Length</b> (m)	<b>Cross-sectional Area</b> (cm <sup>2</sup> )	<b>Concrete Compressive Strength</b> <i>f<sub>c</sub></i> (MPa)	<b>Reinforcement Yield Stress</b> <i>f<sub>y</sub></i> (MPa)	<b>Steel Ratio</b> <i>P<sub>s</sub></i>	<b>Flexural Rigidity</b> (GNm <sup>2</sup> )
1500	34.9	17672	27.5	471	0.025	6.86

#### 1.10 B7 Single Bored (Free and Fixed)

Weight ( $\alpha$ ) of the soil unit was assessed according to fully published cone penetration test results [2]. The tip resistance of the Cone penetration tests was equivalent to an average of 5 MPa throughout first 15 metres in depth. Table3 shows pile characteristics utilised in the BEM analyses.

The pile section's bending moment-rotation relation is compared to the model which may take into account the effect of stress intensification[23].



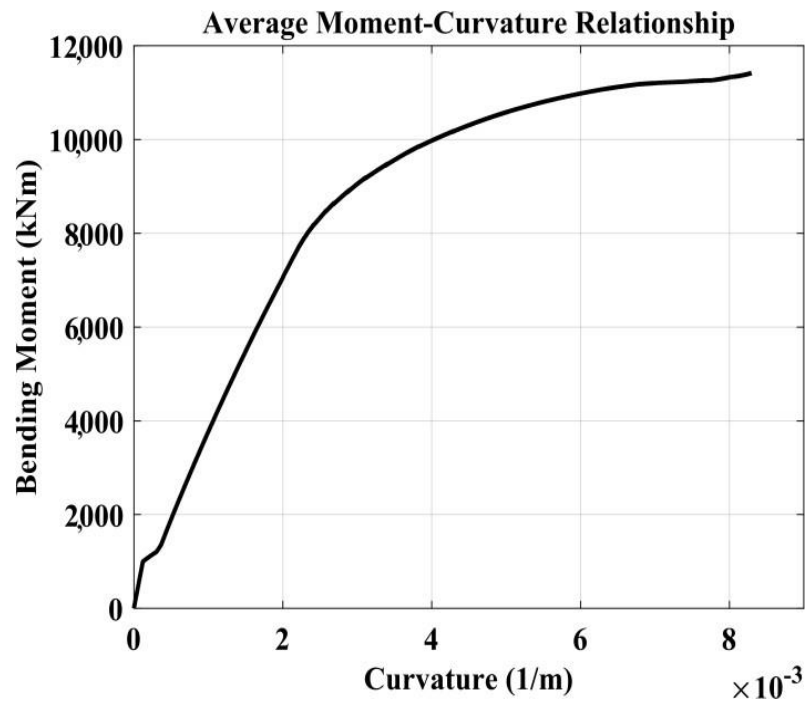


**Figure 11.** For the B7 pile section, the ‘bending moment-curvature’ connection exists.

According to the cone penetration testing findings in[2], an angle of internal friction around 34 was determined by the connection provided [27] .

This was in [2] for the  $G_{max}$  profile. This profile had been reduced from 15 to 150 MPa and is expected to rise linearly. The ratio of Poisson was 0.35.

According to the connection Reese et al. [19], the final soil pressure profile was assessed. Since of the absence of data to apply strictly the Modified Kovacs Model, estimated suction effects were taken into account since the groundwater table was one metre below the surface, which increased vertical and effective soil stress at the first metre. In fact, from zero kPa to ten kPa from one metres deep, a linearly rising suction value has been taken. As a result of this, the ground resistance profile is enhanced at the first metre's depth, as achieved using the connections proposed in [19].

The comparison for free-head single pile example between measured and estimated values is given in Figure14.

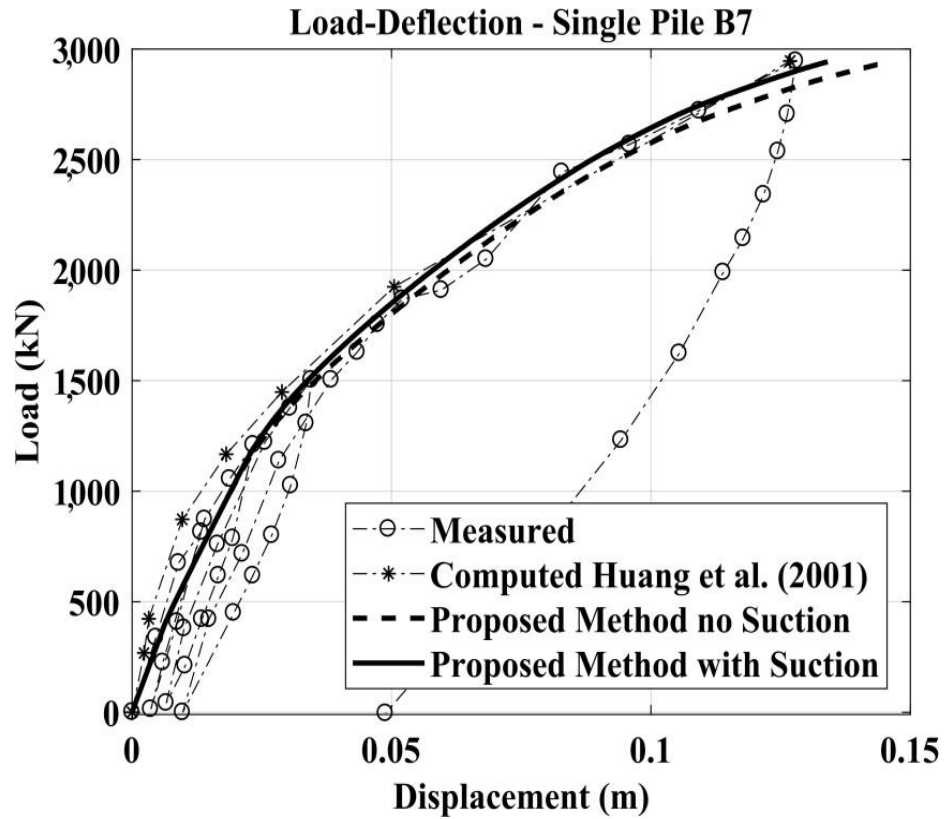


**Figure 12.** Lateral Load versus Head Deflection curve.

BEM has ability to predict horizontally charged pile reaction excellent in all instances, but the prediction of suction may still be improved. The resultant data for the two three, fixed-head pile group, for a given lateral load value for all stacks in the group are shown for the load diffusion curve of a mean stack in group, stack deflection profile.  $H_{group}/(n H_{single})$  is the group efficiency of the stack group analysis findings, where  $H_{group}$  is the pile group total horizontal load. All of the piles' load deflection curves are displayed. The average data for two identical heaps is represented by each curve.

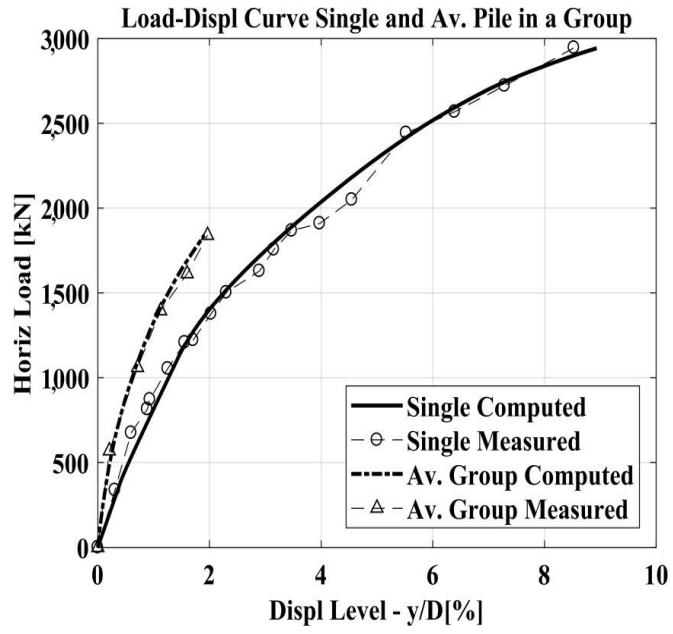


Figure 13. Computed vs. measured load-deflection curves.

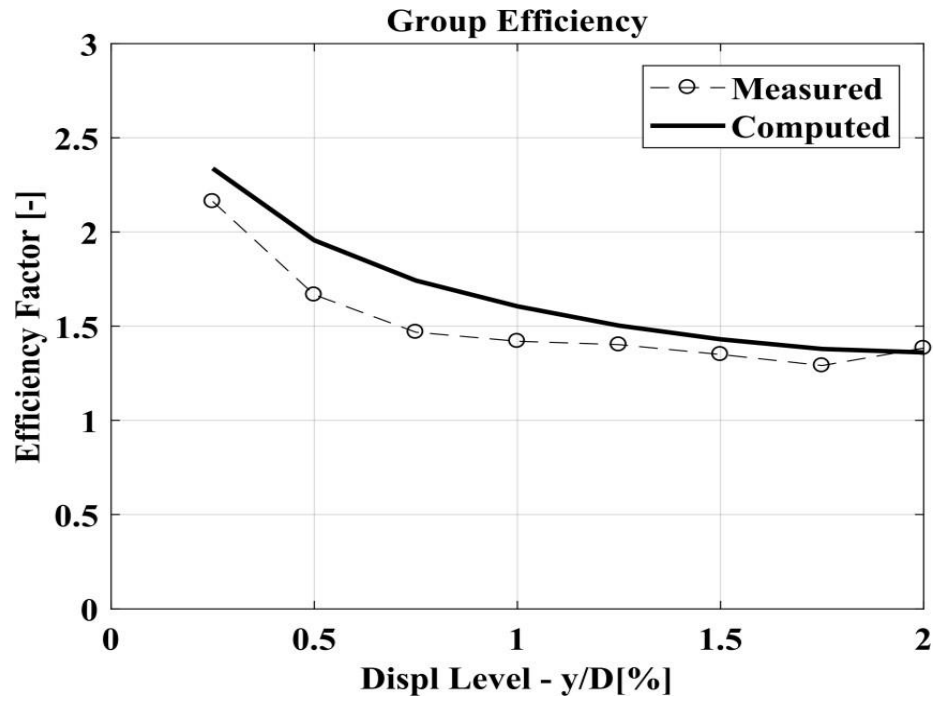


Figure 14. Computed vs. measured group efficiency.

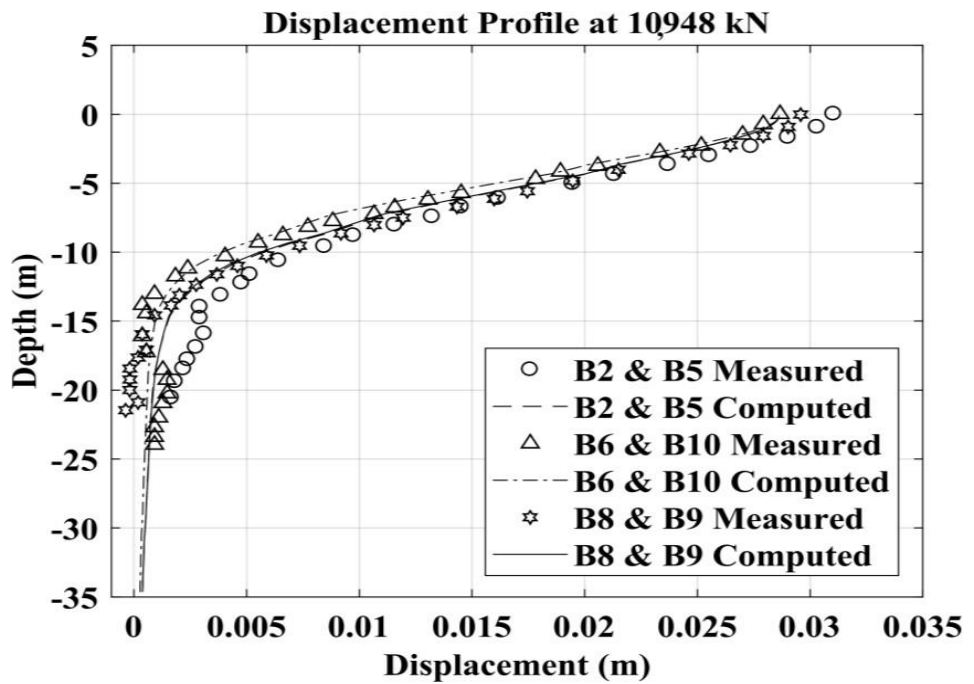


Figure 15. Computed vs. measured deflection profiles

Because the individual stack has been verified , but stack group is fixed head, group efficiency is larger than one in Figure 15. The load of 1462 kN in [2] and [25] was treated as the load lateral breaking moment based on back analysis findings i.e why the corresponding portion of the piles were considered to have decreased bending rigidity in [2] and more recently in [25].

LPILE[57] and VERSAT-P3D[58] were the computer codes utilised in [2] and [23]. However, the suggested BEM method automatically updates bending stiffness of pile block to "average moment curvature" in the real portion of the pile.

With the Intel Core i7 CPU processor on a laptop, calculating the entire lateral load deflection curve takes less than 10 minutes. to get the boring battery group data (2.20 GHz). Analyzes of comparable VERSAT-P3D issues [25] with a simple finite element mesh take approximately 20 min for a one-point displacement calculation, whereas FLAC-3D takes about 6 h [13].

## CONCLUSION

The complex soil-structural interaction (SSI) issue is a piling group which is exposed to horizontal load. Even today, this particular SSI issue cannot be addressed easily, especially since most PC codes are either structural or geotechnical problems to solve/study.

The constant change in relative stiffness between the pile and the earth, while horizontal load, is one of the essential features of the lateral behaviour.

In order to capture the latter, a novel BEM method was devised and verified to analyse the laterally charged pile group. A solution system of the suggested approach for Free Head and Fixed Head instances is given in its entirety, but a different retention condition may be taken into account.

The BEM method presented is unique because the extremely nonlinear conduct of reinforced concrete piles may also be taken into consideration when evaluating the tension-stiffening impact. In addition, in the Modified-Kovacs model, the impact of suction on the high ground layers is taken into account.

Various FDM, FEM, and quasi-3D FEM codes are compared with proposed in this report has two important advantages: reducing the calculation time and making it easy to select/defining the input Parameters to analyse.

The dependability of the suggested BEM technique has been evaluated, using the existing technical literary material on this subject to compare calculated and Full-scale and centrifuge testing of 15 pile groupings yielded the following results.. The findings herein demonstrated the capacity of the BEM approach for excellent prediction of the important features of horizontal behaviour, both qualitatively and quantitatively. For majority of the case

studies, the prediction errors are less than 30 percent.

Finally, the suggested technique was utilised for comparative purposes to horizontally evaluate a certain stacking group loaded in a complete Taiwan testing programme conducted in 2001.



## REFERENCES

1. O'Neill, M.; Dunnavant, T.W. *A Study of the Effects of Scale, Velocity, and Cyclic Degradability on Laterally Loaded Single Piles in Overconsolidated Clay*; University of Houston: Houston, TX, USA, 1984.
2. Huang, A.B.; Hsueh, C.K.; O'Neill, M.W.; Chern, S.; Chen, C. Effects of construction on laterally loaded pile groups. *J. Geotech. Geoenviron. Eng.* **2001**, *127*, 385–397. [CrossRef]  
*J. Geotech. Geoenviron. Eng.* **1998**, *124*, 1016–1026. [CrossRef]
3. *Lateral-Load Tests on 25.4 mm (1-in.) Diameter Piles in Very Soft Clay in Side-by-Side and in-Line Groups*; ASTM: West Conshohocken, PA, USA, 1984; STP 835; pp. 122–139.
4. McVay, M.; Casper, R.; Shang, T.I. Lateral response of three-row groups in loose to dense sands at 3D and 5D pile spacing. *J. Geotech. Eng.* **1995**, *121*, 436–441. [CrossRef]
5. Rollins, K.M.; Gerber, T.M.; Lane, J.D.; Ashford, S.A. Lateral resistance of a full-scale pile group in liquefied sand. *J. Geotech. Geoenviron. Eng.* **2005**, *131*, 115–125. [CrossRef]
6. Mokwa, R. Investigation of the Resistance of Pile Caps to Lateral Loading. PhD Thesis, Virginia Polytechnic and State University, Blacksburg, VA, USA, February 2000.
7. Rollins, K.; Lane, J.; Gerber, T. Measured and computed lateral response of a pile group in sand. *J. Geotech. Geoenviron. Eng.* **2006**, *132*, 103–114. [CrossRef]  
*J. Bridg. Eng.* **1996**, *1*, 135–142. [CrossRef]
8. Abdrabbo, F.M.; Gaaver, K.E. Simplified analysis of laterally loaded pile groups. *Alexandria Eng. J.* **2012**, *51*, 121–127. [CrossRef]
9. *Int. J. Numer. Anal. Methods Geomech.* **2003**, *27*, 1255–1276. [CrossRef]
10. Mindlin, R.D. Force at a point in the interior of a semi-infinite solid. *Physics* **1936**, *7*, 195–202. [CrossRef]

11. Poulos, H.G.; Davis, E.H. *Pile Foundation Analysis and Design*; Wiley & Sons: New York, NY, USA, 1980.
12. Davies, T.G.; Banerjee, P.K. The displacement field due to a point load at the interface of a two layer elastic half-space. *Geotechnique* **1978**, *28*, 43–56. [CrossRef]  
*Can. Geotech. J.* **1986**, *23*, 441–450. [CrossRef]
13. Budhu, M.; Davies, T.G. Nonlinear analysis of laterality loaded piles in cohesionless soils. *Can. Geotech. J.* **1987**, *24*, 289–296. [CrossRef]
14. Matos Filho, R.; Mendonça, A.V.; Paiva, J.B. Static boundary element analysis of piles submitted to horizontal and vertical loads. *Eng. Anal. Bound. Elem.* **2005**, *29*, 195–203. [CrossRef]
15. Small, J.C.; Zhang, H.H. Piled raft foundations subjected to general loadings. In Proceedings of the Developments in Theoretical Geomechanics, Sydney, Australia, 1 January 2000
16. Ashour, M.; Norris, G.; Pilling, P. Lateral Loading of a Pile in Layered Soil Using the Strain Wedge Model. *J. Geotech. Geoenviron. Eng.* **1998**, *124*, 303–315. [CrossRef]  
**2004**, *130*, 580–592. [CrossRef]
17. Fahey, M.; Carter, J. A finite element study of the pressuremeter test in sand using a nonlinear elastic plastic model. *Can. Geotech. J.* **1993**, *30*, 348–362. [CrossRef]
18. Matlock, H. Correlations for design of laterally loaded piles in soft clay. In Proceedings of the 2nd Annual Offshore Technology Conference, Houston, TX, USA, 22–24 April 1970; pp. 577–588.
19. Reese, L.C.; Cox, W.R.; Koop, F.D. Analysis of laterally loaded piles in sand. In Proceedings of the VI Annual Offshore Technology Conference, Houston, TX, USA, 1974; pp. 473–485.
20. Reese, L.; Cox, W.; Koop, F. Field testing and analysis of laterally loaded piles in stiff clay. Proceedings of Offshore Technology Conference, Houston, TX, USA, 5–8 May 1975; pp. 671–690.

21. Landi, G. Pali soggetti a carichi orizzontali: Indagini sperimentali ed analisi. PhD Thesis, University of Naples Federico II, Pisa, Italia, 26–28 June 2006.
22. Stacul, S.; Squeglia, N.; Morelli, F. Laterally Loaded Single Pile Response Considering the Influence of Suction and Non-Linear Behaviour of Reinforced Concrete Sections. *Appl. Sci.* **2017**, *7*, 1310. [CrossRef]
23. Morelli, F.; Amico, C.; Salvatore, W.; Squeglia, N.; Stacul, S. Influence of Tension Stiffening on the Flexural Stiffness of Reinforced Concrete Circular Sections. *Materials* **2017**, *10*, 201. [CrossRef]
24. Press, W.H.; Teukolsky, S.A.; Vetterling, W.T.; Flannery, B.P. *Numerical Recipes in C++*. *The Art of Scientific Computing*, 2nd ed.; Cambridge University Press: Cambridge, UK, 2002; pp. 714–718.
25. Wu, G.; Finn, W.L.; Dowling, J. Quasi-3D analysis: Validation by full 3D analysis and field tests on single piles and pile groups. *Soil Dyn. Earthq. Eng.* **2015**, *78*, 61–70. [CrossRef]
26. Fayyazi, M.S.; Taiebat, M.; Finn, W.L. Group reduction factors for analysis of laterally loaded pile groups. *Can. Geotech. J.* **2014**, *51*, 758–769. [CrossRef]
27. Mayne, P.W. In situ test calibrations for evaluating soil parameters. In Proceedings of the Second International Workshop on Characterisation and Engineering Properties of Natural Soils, Singapore, Singapore, 29 November–1 December 2006; Tan, T.S., Phoon, K.K., Hight, D.W., Leroueil, S., Eds.; CRC Press: Boca Raton, FL, USA; pp. 1601–1652.
28. Aubertin, M.; Mbonimpa, M.; Bussière, B.; Chapuis, R.P. A model to predict the water retention curve from basic geotechnical properties. *Can. Geotech. J.* **2003**, *40*, 1104–1122. [CrossRef]
29. Poulos, H.G.; Davis, E.H. *Pile Foundation Analysis and Design*; Wiley & Sons: New York, NY, USA, 1980.